

Inverse Problem of a Buried Metallic Object

Wei Chien, Chung-Hsin Huang, Chun Jen Lin and Chien-Ching Chiu

Electrical Engineering Department, Tamkang University

Tamsui, Taiwan, R.O.C.

e-mail : chiu@ee.tku.edu.tw phone : +886226215656 # 2737 Fax: +886226209814

Abstract -- In this paper we address an inverse scattering problem whose aim is to discuss the CPU time for recovering a perfectly conducting cylindrical object buried in a half-space. First, we use Fourier-series or cubic-spline methods to describe the shape and reformulate the inverse problem into an optimization one. Then we solved it by the improved Steady State Genetic Algorithm (SSGA) and Simple Genetic Algorithm (SGA) respectively and compare the cost time in finding out the global extreme solution of the objective function. It is found the searching ability of SSGA is much powerful than that of the SGA. Even when the initial guess is far away from the exact one, the cost time for converging to a global extreme solution using by SSGA is much less than that by SGA. Numerical results are given to show that the inverse problem by using SSGA is much better than SGA in time costing.

I. Introduction

Due to the large area of applications such as non-destructive problems, geophysical prospecting and determination of underground tunnels and pipelines, etc., the inverse scattering problems related to the buried bodies are of particular importance in the scattering theory. In the past 20 years, many rigorous methods have been developed to solve the exact equations [1]-[8]. However, inverse problems of this type are difficult to solve because they are ill-posed and nonlinear [9]. As a result, many inverse problems are reformulated into optimization ones and then numerically solved by different iterative methods such as the Newton-Kantorovitch method [1]-[4], the Levenberg-Marquardt algorithm [5]-[7], and the successive-overrelaxation method [8]. Most of these approaches employ the gradient-based searching scheme to find the extreme of the cost function, which are highly dependent on the initial guess and usually get trapped in the local extreme. The GA [10] is an evolutionary algorithm that uses the stochastic mechanism to search

through the parameter space. Although we can get good reconstruction by using SGA to solve the inverse problem, we found that SGA will need a lot of time to get the accurate result, since repeated calculating scattered field will take over the great part of time, especially in half-space inverse problem that Green function converges slowly. As a result, a lot of CPU time is needed to deal with the half-space case. In such a case, it is more suitable by using SSGA, since the features of SSGA are using less function calls (In the inverse problem, function calls mean to calculate the scattered field) to get the same result. In this paper, inverse problem of the half space case solved by an improved SSGA using non-uniform probability density function (pdf) is proposed and compared with SGA. In Section II, a theoretical formulation for the inverse scattering is presented. The general principles of SGA, and the way we applied them to the inverse problem are described. In section III, numerical results for reconstructing objects of different shapes are given. Finally, some conclusions are drawn in Section IV.

II. Theoretical Formulation

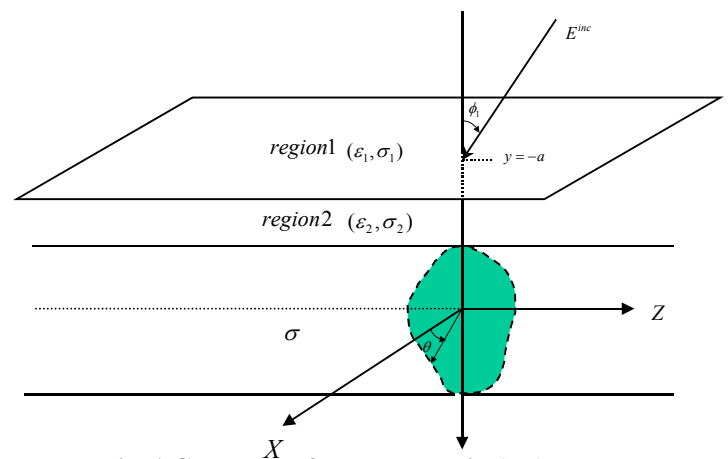


Fig. 1 Geometry of the problem in (x,y) plane.

Let us consider a perfectly conducting cylinder buried in a lossy homogeneous half-space, as shown in Fig 1. The media in regions 1 and 2 are characterized by the permittivities and conductivities (ϵ_1, σ_1) and (ϵ_2, σ_2) , respectively, while the permeability μ_0 is used for each region, i.e., only nonmagnetic media are concerned here. The cross section of the cylinder is described by polar coordinates in the xy plane through the shape function $\rho = F(\theta)$. The cylinder is illuminated by a plane wave with time dependence $\exp(j\omega t)$, of which the electric field is assumed parallel to the Z -axis (i.e., transverse magnetic or TM polarization). Let E^{inc} denote the incident E field from region 1 to region 2 with incident angle ϕ_1 . Owing to the interface between region 1 and region 2, the incident plane wave would generate two waves in the absence of the conducting object: the reflected wave (for $y \leq -a$) and the transmitted wave (for $y > -a$). Thus the unperturbed field is given by

$$\vec{E}_i(\vec{r}) = E_i(x, y)\hat{z} \quad (1)$$

with

$$E_i(x, y) = \begin{cases} E_1(x, y) = e^{-jk_1[x\sin\phi_1 + (y+a)\cos\phi_1]} + R_1 e^{-jk_1[x\sin\phi_1 - (y+a)\cos\phi_1]}, & y \leq -a \\ E_2(x, y) = T e^{-jk_2[x\sin\phi_2 + (y+a)\cos\phi_2]} & , y > -a \end{cases}$$

where

$$R_1 = \frac{1-n}{1+n}, T = \frac{2}{1+n}, n = \frac{\cos\phi_2}{\cos\phi_1} \sqrt{\frac{\epsilon_2 - j\sigma_2/\omega}{\epsilon_1 - j\sigma_1/\omega}}$$

$$k_1 \sin\phi_1 = k_2 \sin\phi_2$$

$$k_i^2 = \omega^2 \epsilon_i \mu_0 - j\omega \mu_0 \sigma_i, i = 1, 2 \quad \text{Im}(k_i) \leq 0$$

According to the equivalent induced current concept, the scattered field can be expressed by

$$E_s(x, y) = -\int_0^{2\pi} G(x, y; F(\theta'), \theta') J(\theta') d\theta' \quad (2)$$

with

$$J(\theta) = -j\omega \mu_0 \sqrt{F^2(\theta) + F'^2(\theta)} J_s(\theta)$$

$$G(x, y; r', \theta') = \begin{cases} G_1(x, y; r', \theta') & , y \leq -a \\ G_2(x, y; r', \theta') = G_f(x, y; r', \theta') + G_s(x, y; r', \theta') & , y > -a \end{cases}$$

$$\text{-----}(3)$$

where

$$G_1(x, y; x', y') = \frac{1}{2\pi} \int_{-\infty}^{\infty} \frac{j}{\gamma_1 + \gamma_2} e^{j\gamma_1(y+a)} e^{-j\gamma_2(y'+a)} e^{-j\alpha(x-x')} d\alpha \text{-----} (3a)$$

$$G_f(x, y; x', y') = \frac{j}{4} H_0^{(2)}[k_2 \sqrt{(x-x')^2 + (y-y')^2}] \text{-----} (3b)$$

$$G_s(x, y; x', y') = \frac{1}{2\pi} \int_{-\infty}^{\infty} \frac{j}{2\gamma_2} \left(\frac{\gamma_2 - \gamma_1}{\gamma_2 + \gamma_1} \right) e^{-j\gamma_2(y+2a+y')} e^{-j\alpha(x-x')} d\alpha \text{-----} (3c)$$

$$\gamma_i^2 = k_i^2 - \alpha^2, i = 1, 2, \text{Im}(\gamma_i) \leq 0, y' > a$$

Note that the same point cause expressed as (r', θ') in polar coordinate or (x', y') in Cartesian coordinate. Here $J_s(\theta)$ is the induced surface current density that is proportional to the normal derivative of the electric field on the conductor surface.

The boundary condition for a perfectly conducting object is

$$\hat{n} \times \vec{E} = 0 \quad (4)$$

where \hat{n} is the outward unit vector normal to the surface of the scatterer. The boundary condition at the surface of the scatterer given by (4) then leads to an integral equation for $J(\theta)$:

$$E_2(F(\theta), \theta) = \int_0^{2\pi} G_2(F(\theta), \theta; F(\theta'), \theta') J(\theta') d\theta' \quad (5)$$

The total field E^{out} in region 1 is given by

$$E^{out}(r) = E_1(r) - \int_0^{2\pi} G_1(r; F(\theta'), \theta') J(\theta') d\theta' \quad (6)$$

The direct problem is to compute the total field in region 1 when the shape function $F(\theta)$ is given. This can be achieved by first solving for J from equation (5) and then calculating E^{out} by equation (6).

Let us consider the following inverse problem: given the scattered electric field E_s measured outside the scatterer, determine the shape function $F(\theta)$ of the object.

III. Numerical Results

Let us consider a perfectly conducting cylinder buried in a lossless half-space ($\sigma_1 = \sigma_2 = 0$). The permittivities in region 1 and region 2 are characterized by $\epsilon_1 = \epsilon_0$ and $\epsilon_2 = 2.56\epsilon_0$, respectively. A TM polarization plane wave of unit amplitude is incident from region 1 upon the object in region 2 as shown in

Fig. 1. The frequency of the incident wave is chosen to be 3GHz, of which the wavelength λ_0 in free space is 0.1m. The object is buried at a depth $a \cong \lambda_0$ and the scattered fields are measured on a probing line along the interface between region 1 and region 2. To reconstruct the shape of the object, the object is illuminated by three incident waves from different directions, while 20 measurement points at equal spacing are used along the interface $y = -a$ for each incident angle. There are 60 measurement points in each simulation.

In both algorithms, the population size are chosen as 100 (i.e. $X=100$). The binary string length of the unknown coefficient, ρ_i is set to be 20 bits (i.e., $L=20$). The search range for the unknown coefficient of the shape function is chosen to be from 0 to 0.1. The extreme value of the coefficient of the shape function can be determined by the prior knowledge of the objects. Here, the prior knowledge means that we can get the approximate position and the size of the buried cylinder by first using tomography technique, and then get the exact solution by the genetic algorithm. The crossover probability p_c is set to be 0.05 in NU-SSGA and 0.5 in SGA. Note that, in a typical GA, it use the crossover and mutation operator to generate all the new population in each new generation. On the contrary, NU-SSGA only need to generate a few new population in each new generation. The mutation probability p_m is set to be 0.5 in both algorithms. The value of β is chosen to be 0.001. The efficient NU-SSGA is then applied to enhance the convergence and increase the converging rate of finding the global extreme of the inverse scattering problems.

The maximum number of generation is set 1000 in SGA and 5000 in NU-SSGA. However, when the change of fitness value is less than 1% in 500 generations, the simulation will also stop.

In the first example, the shape function is selected by the cubic-spline expand to be $\rho_0 = 0.02$ m, $\rho_1 = 0.02 \times \sqrt{3}$ m, $\rho_2 = 0.02 \times \sqrt{3}$ m, $\rho_3 = 0.02$ m, $\rho_4 = 0.02 \times \sqrt{3}$ m and $\rho_5 = 0.02 \times \sqrt{3}$ m. Here, the spline ranges are defined as $h_1 = \theta_1 - \theta_0$, $h_2 = \theta_2 - \theta_1, \dots$ and $h_n = \theta_n - \theta_{n-1}$. We set the same spline range to expand the shape in the simulation. In this example, the cubic-spline expand is also chosen to recover the shape function. The reconstructed shape function at 6000 function call using

by SGA and NU-SSGA are plotted in Fig. 5(a) respectively with the relative errors shown in Fig. 5(b). Here DR, which is called shape function discrepancy respectively, are defined as

$$DR = \left\{ \frac{1}{N'} \sum_{i=1}^{N'} [F^{cal}(\theta_i) - F(\theta_i)]^2 / F^2(\theta_i) \right\}^{1/2} \quad (7)$$

where N' is set to 60. The quantities DR provides measures of how well $F^{cal}(\theta)$ approximates $F(\theta)$ respectively. From Fig. 2(a) and Fig. 2(b), it is clear that the efficiency of the NU-SSGA is much better than that of SGA. We can save more than 90% CPU time by using NU-SSGA. To investigate the sensitivity of the imaging algorithm against random noise, two independent Gaussian noises with zero mean have been added to the real and imaginary parts of the simulated scattered fields. We use the normalized standard deviations of 10^{-2} to test the SGA and NU-SSGA. The normalized standard deviation is defined as the standard deviation of the Gaussian noise divided by the rms value of the scattered fields. Here, the signal-to-noise ratio (SNR) is inversely proportional to the normalized standard deviation. The numerical result is plotted in Fig. 2(c).

IV. Conclusions

We have presented a study of comparing the efficiency of the SGA and NU-SSGA to reconstruct the shape of a buried metallic object through knowledge of scattered field. Based on the boundary condition and measured scattered field, we have derived a set of nonlinear integral equations and reformulated the imaging problem into an optimization problem. Besides, the contours of the cylinders are expanded by the cubic-spline for the inverse problem instead of the trigonometric series to guarantee the nonnegative definition of the shape. Experiment results show that the searching ability and efficiency of NU-SSGA are much powerful than that of SGA. We can save more than 90% CPU time to get the satisfied result for all the examples.

Acknowledgment

This work was supported by National Science Council, Republic of China, under Grant NSC-91-2219-E-032-004.

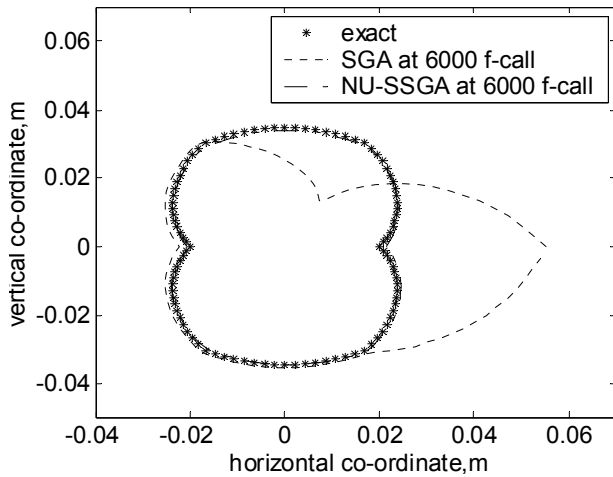


Fig. 2 (a) Shape function for example. The star curve represents the exact shape, while the curves of short and long imaginary lines are the results at 6000 function call by using SGA and NU-SSGA respectively.

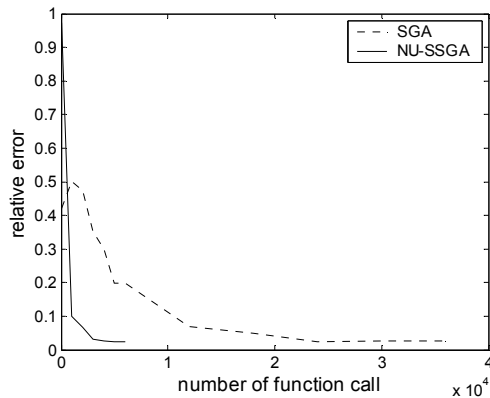


Fig. 2 (b) The trend of relative error for SGA and NU-SSGA method.

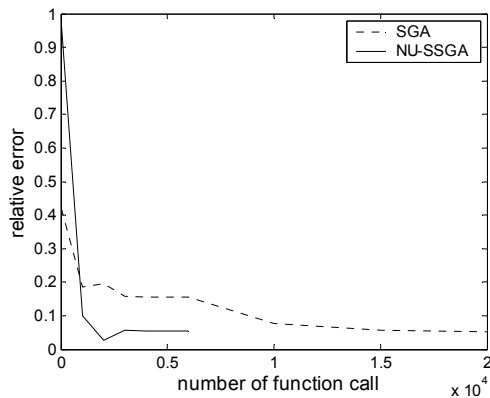


Fig. 2 (c) The trend of relative error for SGA and NU-SSGA method with noise level at 10^{-2} .

V. References

- [1] A. Roger, "Newton-Kantorovitch algorithm applied to an electromagnetic inverse problem," *IEEE Trans. Antennas Propagat.*, vol. AP-29, pp. 232-238, Mar. 1981.
- [2] C. C. Chiu and Y. W. Kiang, "Inverse scattering of a buried conducting cylinder," *Inverse Problems*, vol. 7, pp. 187-202, April 1991.
- [3] C. C. Chiu and Y. W. Kiang, "Microwave imaging of multiple conducting cylinders," *IEEE Trans. Antennas Propagat.*, vol. 40, pp. 933-941, Aug. 1992.
- [4] G. P. Otto and W. C. Chew, "Microwave inverse scattering-local shape function imaging for improved resolution of strong scatterers." *IEEE Trans. Microwave Theory Tech.*, vol. 42, pp. 137-142, Jan. 1994.
- [5] D. Colton and P. Monk, "A novel method for solving the inverse scattering problem for time-harmonic acoustic waves in the resonance region II," *SIAM J. Appl. Math.*, vol. 46, pp. 506-523, June 1986.
- [6] A. Kirsch, R. Kress, P. Monk, and A. Zinn, "Two methods for solving the inverse acoustic scattering problem," *Inverse problems*, vol. 4, pp. 749-770, Aug. 1998.
- [7] F. Hettlich, "Two methods for solving an inverse conductive scattering problem," *Inverse Problems*, vol. 10, pp. 375-385, 1994.
- [8] R. E. Kleinman and P.M. van den Berg, "Two-dimensional location and shape reconstruction," *Radio Sci.*, vol. 29, pp. 1157-1169, July-Aug. 1994.
- [9] Hohage T, "Iterative methods in inverse obstacle scattering: regularization theory of linear and nonlinear exponentially ill-posed problems," Dissertation Linz, 1999.
- [10] D. E. Goldberg, Genetic Algorithm in Search, Optimization and Machine Learning, Addison-Wesley, 1989.
- [11] E.C. Jordan and K.G. Balmain, Electromagnetic Waves and Radiating systems. Englewood Cliffs, NJ: Prentice-Hall, 1968.
- [12] Shoichiro Nakamura, "Applied Numerical Method in C," Prentice-Hall int. 1993
- [13] "A practical Guide to Splines," New York: Spring-Verlag, 1987.
- [14] S. Weile, and E. Michielssen, "Genetic algorithm optimization applied to electromagnetics: a review", *IEEE Trans. Antennas and Propagation*, Vol. 45, pp. 343-353, 1997.